

# Impact of the Low Temperature Ohmic Contact Process on DC and Forward Gate Bias Stress Operation of GaN HEMT Devices

Oguz Odabasi<sup>1</sup>, Amir Ghobadi<sup>1</sup>, Turkan Gamze Ulusoy Ghobadi, Yakup Unal, Gurur Salkim, Gunes Basar, Bayram Butun<sup>1</sup>, and Ekmel Ozbay<sup>1</sup>

**Abstract**—In AlGaIn/GaN high electron mobility transistors (HEMTs), high temperature processes (such as ohmic annealing with  $>800^{\circ}\text{C}$  value) could deform the crystal structure and induce trap states within the bulk and surface. Expanded defect densities cause crucial problems, such as threshold voltage ( $V_{th}$ ) instability, current collapse, and high leakages. In this work, a low temperature ohmic contact process ( $630^{\circ}\text{C}$ , 10 minutes) is adopted with recess etch, and contact resistances  $<0.1\ \Omega \cdot \text{mm}$  with low sheet resistances are achieved. The positive impact of this low thermal budget process on surface morphology, DC operation, long-term stability, and forward gate bias stress of the device is studied.

**Index Terms**—AlGaIn/GaN HEMTs, ohmic contact, stability, surface roughness, annealing temperatures, recessed ohmic contacts.

## I. INTRODUCTION

AlGaIn/GaN HEMTs are the perfect option for high frequency and high power applications due to the high current capability and electron velocity [1], [2]. Ohmic contact formation is a fundamental step in device fabrication. Especially for high frequency power amplifiers, parasitic resistances have a high impact on RF performance and output

Manuscript received 4 June 2022; revised 25 July 2022; accepted 8 August 2022. Date of publication 17 August 2022; date of current version 27 September 2022. This work was supported in part by the Turkish Scientific and Technological Research Council, the Scientific and Technological Research Council of Türkiye (TUBITAK), under 1501 Project GaNTURK; and in part by Turkcell Technology within the Framework of the Fifth Generation (5G) and Beyond Joint Graduate Support Program Coordinated by the Information and Communication Technologies Authority. The work of Ekmel Ozbay was supported by the Turkish Academy of Sciences. The review of this letter was arranged by Editor V. Misra. (Corresponding author: Amir Ghobadi.)

Oguz Odabasi is with the Nanotechnology Research Center (NANOTAM), Department of Electrical and Electronics Engineering, Bilkent University, 06800 Ankara, Turkey, and also with Turkcell Technology, 34854 Istanbul, Turkey.

Amir Ghobadi, Yakup Unal, Gurur Salkim, Gunes Basar, and Bayram Butun are with the Nanotechnology Research Center (NANOTAM), Bilkent University, 06800 Ankara, Turkey (e-mail: amir.ghobadi.ee@gmail.com).

Turkan Gamze Ulusoy Ghobadi is with the Nanotechnology Research Center, Bilkent University, 06800 Ankara, Turkey.

Ekmel Ozbay is with the Nanotechnology Research Center (NANOTAM), Department of Electrical and Electronics Engineering, and the Department of Physics, Institute of Materials Science and Nanotechnology (UNAM), Bilkent University, 06800 Ankara, Turkey.

Color versions of one or more figures in this letter are available at <https://doi.org/10.1109/LED.2022.3199569>.

Digital Object Identifier 10.1109/LED.2022.3199569

power [3]. However, to get low contact resistance ( $R_c$ ), high temperature annealing is commonly used. [4]. For GaN HEMT, a typical ohmic contact metallization is formed as Ti/Al/Ni/Au stacks [5]. Ti removes the surface oxide and Al diffuses into the bulk to form conductive paths by forming Al-N bonds. The created nitrogen deficiency causes high doping in the contact region, which lowers the barrier and forms an ohmic contact [6]. Ni is also used as a diffusion barrier between the Au and Al layers [7]. Although this approach achieved very low ohmic resistances, it requires very high thermal cycles, might increase to  $850^{\circ}\text{C}$ , and forms alloys and spikes [8]. Such high temperatures can distort GaN crystal and increase the trap densities [9]. In addition, it can cause strain relaxation and reduce the electron density of two-dimensional electron gas (2-DEG) [10].

To address this issue, much effort has been recently devoted to the realization of low temperature ohmic contacts [11]. Tantalum-based ohmic contacts are shown to achieve  $0.24\ \Omega \cdot \text{mm}$  at  $500^{\circ}\text{C}$  [12]. Tungsten (W) based stacks lowered the  $R_c$  down to  $0.35\ \Omega \cdot \text{mm}$  with  $500^{\circ}\text{C}$  annealing [13], [14]. However, having a high melting point, W is a hard material for physical vapor deposition (PVD) systems, which is mainly used for most foundries. Ion implantation can provide  $0.4\ \Omega \cdot \text{mm}$   $R_c$ , but post annealing is required to activate the implanted ions [15], [16]. The implementation of MBE or MOCVD growth highly doped (n+) regions for low ohmic contact resistances is also commonly used in highly scaled devices. Low ohmic contact resistances can be achieved without additional annealing due to a high carrier concentration at the regrown region. However, this method requires the sample to enter the MBE or MOCVD chamber after being processed, which can cause contamination in the chamber. It is also relatively expensive and harder to implement. [17]. Among all, the recess etch approach is proven to achieve contact resistances as low as  $0.2\ \Omega \cdot \text{mm}$  at low temperatures [12], [18], [19]. Although much effort has been spent on achieving low contact resistances with minimal thermal budgets, there are very limited studies on the impact of this factor on DC, long-term, and forward gate stress operation of GaN HEMTs. Especially, under a forward bias gate turn on, when a large current density flows, the trapping effects become highly detrimental.

In the present letter, we first develop a recessed low temperature ohmic contact based on Ti/Al/Ni/Au to achieve  $<0.1\ \Omega \cdot \text{mm}$   $R_c$ , based on the process described in [19],

which is one of the smallest reported values so far. Later, conventional high temperature ohmic contacts and the proposed design are brought into HEMT devices. Fabricated devices are tested for surface morphology, DC operation, stability, and forward bias stress conditions. It is found that devices with low temperature ohmic contacts have lower sheet resistance, lower gate leakage currents, and more stable response to DC and long-term stress than a conventional one. Moreover, under forward gate bias stress (which is an important factor for RF amplifiers' large-signal operation), the low temperature HEMT has almost no change in quiescent drain current ( $I_{DQ}$ ), in gate biases as large as 4 V.

## II. EPITAXIAL-GROWTH AND DEVICE DETAILS

An AlGaIn/GaN HEMT epitaxy structure was grown on a 4-H SiC substrate using a metal organic chemical vapor deposition (MOCVD) system. On C-doped GaN buffer, 20 nm AlN nucleation, 200 nm transition and 130 nm channel GaN, 1 nm AlN spike, and 20 nm thick  $\text{Al}_{0.22}\text{Ga}_{0.78}\text{N}$  barrier layers were grown, respectively. Electron mobility ( $\mu_n$ ) and concentration ( $n_s$ ) are  $2,000 \text{ cm}^2/\text{V}\cdot\text{s}$  and  $1.1 \times 10^{13} \text{ cm}^{-2}$ , respectively. The sheet resistance ( $R_{sh}$ ) of the as-grown HEMT structure was measured as  $310 \Omega/\square$ . For mesa isolation, 100 nm Cl-based etching was used via inductively coupled plasma reactive ion etching (ICP-RIE) on patterns defined by optical lithography. Alloyed ohmic contacts were used for reference devices. Ti/Al/Ni/Au metal stack was deposited by an e-beam evaporator with 12 nm/100 nm/50 nm/50 nm thicknesses, respectively.  $830^\circ\text{C}$ , 30 s rapid thermal annealing was applied in a nitrogen environment for ohmic contact formation.

For the low temperature ohmic contacts, a recess etch was applied by ICP-RIE. A 22 nm etch was achieved by using  $\text{BCl}_3/\text{Cl}_2$  chemistry with low RF power (5 W) to minimize the etching-related damages and to increase the process controllability. After the recess etching, samples were cleaned by using diluted HCl (1:10 water) to smooth away etching residues. A Ti/Al/Ni/Au metal stack was deposited by using an e-beam evaporator, in which the only difference with the reference metal stack was the thickness of the Ti and Al layers. A 3 nm of Ti and 140 nm of Al were deposited while Ni and Au thicknesses were kept the same. These devices were annealed at  $630^\circ\text{C}$  for 10 minutes in an N-environment in a rapid thermal annealing chamber.

## III. RESULTS AND DISCUSSION

$R_c$  and  $R_{sh}$  measurements were taken from the transfer length method (TLM) patterns with a  $200 \mu\text{m}$  width and different spacing. The spacings of patterns are verified by using a scanning electron microscope after fabrication. The linear fit of measurements from several patterns was used to calculate the  $R_c$  and  $R_{sh}$ . TLM patterns were isolated from the rest of the sample by a 100 nm mesa etch. The measured data for the conventional and low temperature ohmic contacts are provided in Fig. 1 (a, b). The linear fit of the total resistances of several channel-distanced ohmic contacts perfectly matches the data for both high temperature ohmic contact and low temperature ohmic contact in Fig. 1 (a). Low temperature ohmic contact shows an  $R_{sh}$  of  $350 \Omega/\square$  and  $R_c$  of  $0.078 \text{ Ohm}\cdot\text{mm}$ , while these are found to be  $430 \Omega/\square$  and  $R_c$

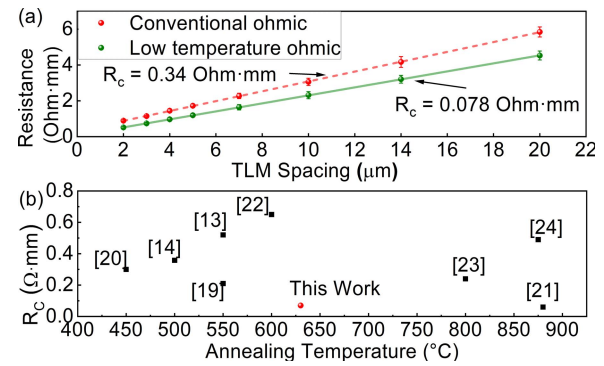


Fig. 1. (a) TLM measurement results with measurement error bars and linear fits of low temperature ohmic contacts and reference contacts, (b) comparison of  $R_c$  and anneal temperature of Ti/Al-based annealed ohmic contacts in the literature.

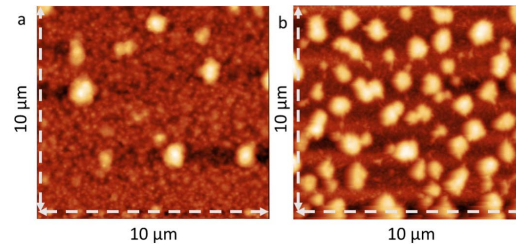


Fig. 2. AFM measurements from (a) low temperature ohmic contact and (b) reference device.

of  $0.34 \text{ Ohm}\cdot\text{mm}$  for conventional HEMT. A contact resistivity of  $2.73 \times 10^{-7} \text{ ohm}\cdot\text{cm}^2$  is calculated for the low temperature ohmic contacts. The reduction in ohmic contact resistances compared to [19] can be associated with the implementation of Au in the metal stack instead of TiN and a slightly higher annealing temperature.

Besides lower  $R_c$ , exposing GaN HEMT to lower temperatures mitigated the formation of surface traps, and this, in turn, shows its impact as lower  $R_{sh}$ . Hall effect measurements also gave 15% higher conductivity in low temperature annealed samples compared to high temperature annealed ones. In Fig. 2 (b), the achieved  $R_c$  with the proposed method is compared with the previously reported work.  $R_c$  of this work is below any reported contact resistance at the below 700-degree range.

Surface roughness is another figure of merit for ohmic contacts. Smoother contact surfaces are desired to prevent device failure, which is related to the long-term diffusion phenomena [25]. Furthermore, it is an important issue in scaling down considerations [26]. Based on the literature, contact with a higher Al/Ti ratio tends to have rougher and bumpy surfaces, although a higher Al/Ti ratio enables lower anneal temperatures [27]. To analyze the surface morphology, atomic force microscopy (AFM) is used in AC surface mode. Fig. 2 (a, b) shows the results of low and high temperature ohmic contacts for a  $10 \mu\text{m} \times 10 \mu\text{m}$  area, respectively. The surface of a high temperature sample is rougher, mainly due to alloy formation between gold and aluminum [28]. On the other hand, a low temperature contact surface is quite smooth with sparse bumps. This can also be seen in the numbers. Low temperature ohmic contact has 42 nm surface roughness, while the high temperature one has 104 nm surface roughness.

After surface characterization, to understand the impact of this process on transistor performance, GaN HEMT devices

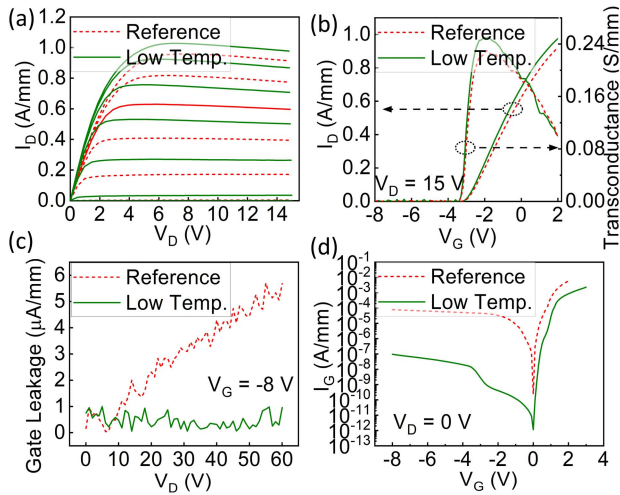


**Fig. 3.** (a)  $I_D$  vs.  $V_D$  measurement for  $V_G$  from  $-8$  V to  $1$  V with  $1$  V steps, (b)  $I_D$  vs.  $V_G$  measurement for  $V_D = 15$  V, (c)  $I_G$  vs.  $V_D$  measurements when  $V_G = -8$  V, (d)  $I_G$  vs.  $V_G$  when the drain contact is grounded, of low temperature ohmic contact and reference devices.

were fabricated. Device fabrication for both reference and low temperature ohmic contact samples are identical except for ohmic contact formation.  $75$  nm SiN was deposited by plasma-enhanced chemical vapor deposition (PECVD) after the mesa etch and ohmic contact formation steps. Therefore, both samples have identical passivation that enables the observation of the effects of the ohmic contact formation process. To define the gate patterns, E-beam lithography (EBL) was used with  $100$  keV. F-based chemistry was used in ICP-RIE for SiN etching.  $O_2$  descum was applied before gate metal deposition to clean the resist residues.  $50$  nm Ni and  $300$  nm Au were deposited via an e-beam evaporator as gate metal. Devices have a  $5$   $\mu$ m drain to source distance. Gate has a  $500$  nm foot and an  $800$  nm gate connected field plate, which is also named gate head. The gate to source and gate to drain distances are  $2$   $\mu$ m and  $2.75$   $\mu$ m, respectively. Every device has 2 fingers with a  $250$   $\mu$ m total gate periphery.

The  $I_D$ - $V_D$  characteristics of both devices for different gate voltages ( $V_G$ ) are plotted in Fig. 3 (a). For  $0$  V gate bias, improvement in  $R_{on}$  from  $1.92$  Ohm-mm to  $1.53$  Ohm-mm and an increase of the drain saturation current ( $I_{DSS}$ ) from  $0.95$  A/mm to  $1.03$  A/mm are observed in the low temperature device compared to the reference device, in line with  $R_c$  and  $R_{sh}$  reduction. As shown in Fig. 3 (b), low temperature HEMT shows a higher maximum transconductance ( $g_m$ ), which is desired for high frequency operation. Moreover, the proposed design has a lower and  $V_D$  invariant gate leakage current at all measured  $V_D$  values (Fig. 3 (c)), which offers higher long-term stability. A better leakage and diode turn-on performance can be also seen from the  $I_G$ - $V_G$  characteristics of the samples, see Fig. 3 (c). This better Schottky performance and low reverse current prove again the fact that the low temperature process reduces the density of generated bulk and surface traps. This, in turn, leads to a stable and long-term operation of the design [29].

Proposed and reference devices are biased under  $V_D = 40$  V.  $V_G$  was tuned to flow the same amount of current initially and the biasing was kept constant. Because there was an insignificant  $V_{TH}$  difference between devices, the  $V_G$  was nearly the same. The change of the current with

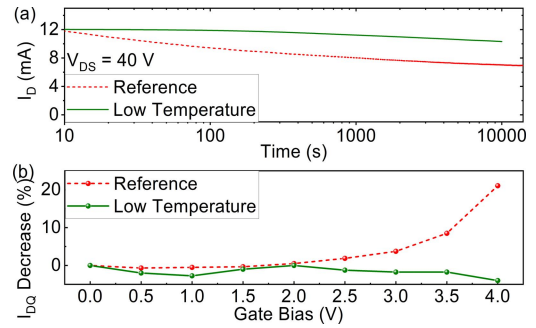


**Fig. 4.** (a) Long-term  $I_D$  measurements, (b) forward gate bias  $I_{DQ}$  measurements, of low temperature ohmic and reference devices.

time was recorded. As can be seen in Fig. 4 (a), a device with low temperature ohmic contacts only experienced a  $1.7$  mA  $I_D$  decrease, which corresponds to  $14\%$ , while this was  $5.1$  mA,  $42\%$  for the reference sample.

The stability of  $I_D$  under device operation conditions is an important factor that is satisfied in the proposed design. However, under RF operation, the device experiences positive  $V_G$  while  $V_D$  is nearly zero volts due to RF swing, which resembles the gate forward current measurements.  $V_{TH}$  instability causes a change in the biasing point of the RF signal that can result in instabilities in the output power and turning off the device due to a positive  $V_{th}$  shift in extreme cases [30]. To have a better qualitative comparison, their turn-on stress operation is studied.

Consecutive DC measurements by a stressing gate with a positive bias and returning to operation voltage are taken from each device and the quiescent drain current ( $I_{DQ}$ ) is compared with the initial value. The change in  $I_{DQ}$  after these measurements are plotted with respect to the maximum gate voltage in Fig. 4 (b). The device with low temperature ohmic contact showed less than a  $5\%$  change in  $I_{DQ}$  up to  $4$  V forward gate bias, which indicates that there is still room for improvement. However, the reference device sees a  $20\%$  decrease in  $I_{DQ}$ . When the gate is turned on, gate current flows and fills the acceptor type of traps in the vicinity of the gate contact, which leads to a threshold voltage shift. In our proposed device, this effect is minimized due to the reduction of the formation of trap states.

#### IV. CONCLUSION

In the present letter,  $<0.1$  Ohm-mm ohmic contact resistance is achieved on GaN/AlGaN/GaN epitaxy by using recess etch and the low temperature anneal process. It is shown that the low temperature improved the sheet resistance. Surface roughness is also decreased in ohmic contacts. GaN HEMT devices are fabricated to test the effect of the proposed contacts on device performance. A combination of a decrease in  $R_{on}$  and gate leakages with improvement in transconductance is observed. Long-term DC tests and forward bias gate measurements showed that the devices with proposed ohmic contacts are more stable and reliable under DC operation.

#### REFERENCES

- [1] U. K. Mishra, L. Shen, T. E. Kazior, and Y.-F. Wu, "GaN-based RF power devices and amplifiers," *Proc. IEEE*, vol. 96, no. 2, pp. 287–305, Feb. 2008, doi: 10.1109/JPROC.2007.911060.

- [2] N. Ikeda, Y. Niiyama, H. Kambayashi, Y. Sato, T. Nomura, S. Kato, and S. Yoshida, "GaN power transistors on Si substrates for switching applications," *Proc. IEEE*, vol. 98, no. 7, pp. 1151–1161, Jul. 2010, doi: [10.1109/JPROC.2009.2034397](https://doi.org/10.1109/JPROC.2009.2034397).
- [3] L. Kolaklieva and R. Kakanakov, "Ohmic contacts for high power and high temperature microelectronics," in *Micro Electronic and Mechanical Systems*. London, U.K.: IntechOpen, Dec. 2009, doi: [10.5772/7017](https://doi.org/10.5772/7017).
- [4] Z. Fan, S. N. Mohammad, W. Kim, Ö. Aktas, A. E. Botchkarev, and H. Morkoç, "Very low resistance multilayer ohmic contact to n-GaN," *Appl. Phys. Lett.*, vol. 68, no. 12, pp. 1672–1674, Mar. 1996, doi: [10.1063/1.115901](https://doi.org/10.1063/1.115901).
- [5] T. Palacios, A. Chakraborty, S. Rajan, C. Poblenz, S. Keller, S. P. DenBaars, J. S. Speck, and U. K. Mishra, "High-power AlGaIn/GaN HEMTs for Ka-band applications," *IEEE Electron Device Lett.*, vol. 26, no. 11, pp. 781–783, Nov. 2005, doi: [10.1109/LED.2005.8577017](https://doi.org/10.1109/LED.2005.8577017).
- [6] D. H. Zadeh, S. Tanabe, N. Watanabe, and H. Matsuzaki, "Characterization of interface reaction of Ti/Al-based ohmic contacts on AlGaIn/GaN epitaxial layers on GaN substrate," *Jpn. J. Appl. Phys.*, vol. 55, no. 5S, Apr. 2016, Art. no. 05FH06, doi: [10.7567/jjap.55.05fh06](https://doi.org/10.7567/jjap.55.05fh06).
- [7] G. Greco, F. Iucolano, and F. Roccaforte, "Ohmic contacts to gallium nitride materials," *Appl. Surf. Sci.*, vol. 383, pp. 324–345, Oct. 2016, doi: [10.1016/j.apsusc.2016.04.016](https://doi.org/10.1016/j.apsusc.2016.04.016).
- [8] Y. Liu, "Recent research on ohmic contacts on GaN-based materials," *IOP Conf. Ser., Mater. Sci. Eng.*, vol. 738, Jan. 2020, Art. no. 012007, doi: [10.1088/1757-899x/738/1/012007](https://doi.org/10.1088/1757-899x/738/1/012007).
- [9] I. Boturchuk, L. Scheffler, A. N. Larsen, and B. Julsgaard, "Evolution of electrically active defects in n-GaN during heat treatment typical for ohmic contact formation," *Phys. Status Solidi A*, vol. 215, no. 9, May 2018, Art. no. 1700516, doi: [10.1002/pssa.201700516](https://doi.org/10.1002/pssa.201700516).
- [10] D. J. Chen, K. X. Zhang, Y. Q. Tao, X. S. Wu, J. Xu, R. Zhang, Y. D. Zheng, and B. Shen, "Temperature-dependent strain relaxation of the AlGaIn barrier in AlGaIn/GaN heterostructures with and without Si<sub>3</sub>N<sub>4</sub> surface passivation," *Appl. Phys. Lett.*, vol. 88, no. 10, Mar. 2006, Art. no. 102106, doi: [10.1063/1.2186369](https://doi.org/10.1063/1.2186369).
- [11] J. He, W. Cheng, Q. Wang, K. Cheng, H. Yu, and Y. Chai, "Recent advances in GaN-based power HEMT devices," *Adv. Electron. Mater.*, vol. 7, no. 4, Apr. 2021, Art. no. 2001045, doi: [10.1080/aeml.202001045](https://doi.org/10.1080/aeml.202001045).
- [12] Y.-K. Lin, J. Bergsten, H. Leong, A. Malmros, J.-T. Chen, D.-Y. Chen, O. Kordina, H. Zirath, E. Y. Chang, and N. Rorsman, "A versatile low-resistance ohmic contact process with ohmic recess and low-temperature annealing for GaN HEMTs," *Semicond. Sci. Technol.*, vol. 33, no. 9, Aug. 2018, Art. no. 095019, doi: [10.1088/1361-6641/aad7a8](https://doi.org/10.1088/1361-6641/aad7a8).
- [13] X. Wang, H.-C. Huang, B. Green, X. Gao, D. Rosenmann, X. Li, and J. Shi, "Au-free low-temperature ohmic contacts for AlGaIn/AlN/GaN heterostructures," *J. Vac. Sci. Technol. B, Microelectron.*, vol. 38, no. 6, Nov. 2020, Art. no. 062206, doi: [10.1116/6.0000287](https://doi.org/10.1116/6.0000287).
- [14] T. Yoshida and T. Egawa, "Improvement of Au-free, Ti/Al/W ohmic contact on AlGaIn/GaN heterostructure featuring a Thin-Ti layer and low temperature annealing," *Phys. Status Solidi A*, vol. 215, no. 13, Feb. 2018, Art. no. 1700825, doi: [10.1002/pssa.201700825](https://doi.org/10.1002/pssa.201700825).
- [15] H. Yu, L. McCarthy, S. Rajan, S. Keller, S. Denbaars, J. Speck, and U. Mishra, "Ion implanted AlGaIn-GaN HEMTs with nonalloyed ohmic contacts," *IEEE Electron Device Lett.*, vol. 26, no. 5, pp. 283–285, May 2005, doi: [10.1109/LED.2005.846583](https://doi.org/10.1109/LED.2005.846583).
- [16] F. Recht, L. McCarthy, S. Rajan, A. Chakraborty, C. Poblenz, A. Corrión, J. S. Speck, and U. K. Mishra, "Nonalloyed ohmic contacts in AlGaIn/GaN HEMTs by ion implantation with reduced activation annealing temperature," *IEEE Electron Device Lett.*, vol. 27, no. 4, pp. 205–207, Apr. 2006, doi: [10.1109/LED.2006.870419](https://doi.org/10.1109/LED.2006.870419).
- [17] J. Guo, G. Li, F. Faria, Y. Cao, R. Wang, J. Verma, X. Gao, S. Guo, E. Beam, A. Ketterson, M. Schuette, P. Saunier, M. Wistey, D. Jena, and H. Xing, "MBE-regrown ohmics in InAlN HEMTs with a regrowth interface resistance of 0.05  $\Omega$ -mm," *IEEE Electron Device Lett.*, vol. 33, no. 4, pp. 525–527, Apr. 2012, doi: [10.1109/LED.2012.2186116](https://doi.org/10.1109/LED.2012.2186116).
- [18] W. S. Lau, J. B. H. Tan, and B. P. Singh, "Formation of ohmic contacts in AlGaIn/GaN HEMT structures at 500°C by ohmic contact recess etching," *Microelectron. Rel.*, vol. 49, no. 5, pp. 558–561, May 2009, doi: [10.1016/j.microrel.2009.02.010](https://doi.org/10.1016/j.microrel.2009.02.010).
- [19] J. Zhang, X. Kang, X. Wang, S. Huang, C. Chen, K. Wei, and X. Liu, "Ultralow-contact-resistance Au-free ohmic contacts with low annealing temperature on AlGaIn/GaN heterostructures," *IEEE Electron Device Lett.*, vol. 39, no. 6, pp. 847–850, Jun. 2018, doi: [10.1109/LED.2018.2822659](https://doi.org/10.1109/LED.2018.2822659).
- [20] Z. Liu, M. Heuken, D. Fahlé, G. I. Ng, and T. Palacios, "CMOS-compatible Ti/Al ohmic contacts ( $R_c < 0.3 \Omega\text{mm}$ ) for u-AlGaIn/AlN/GaN HEMTs by low temperature annealing ( $< 450^\circ\text{C}$ )," in *Proc. 72nd Device Res. Conf.*, Jun. 2014, pp. 75–76, doi: [10.1109/DRC.2014.6872304](https://doi.org/10.1109/DRC.2014.6872304).
- [21] M. Y. Fan, G. Y. Yang, G. N. Zhou, Y. Jiang, W. M. Li, Y. L. Jiang, and H. Y. Yu, "Ultra-low contact resistivity of  $< 0.1 \Omega\text{mm}$  for Au-free Ti<sub>x</sub>Al<sub>y</sub> alloy contact on non-recessed i-AlGaIn/GaN," *IEEE Electron Device Lett.*, vol. 41, no. 1, pp. 143–146, Jan. 2020, doi: [10.1109/LED.2019.2953077](https://doi.org/10.1109/LED.2019.2953077).
- [22] M. Van Hove, X. Kang, S. Stoffels, D. Wellekens, N. Ronchi, and R. Venegas, "Fabrication and performance of au-free AlGaIn/GaN-on-Silicon power devices with Al<sub>2</sub>O<sub>3</sub> and Si<sub>3</sub>N<sub>4</sub>/Al<sub>2</sub>O<sub>3</sub> gate dielectrics," *IEEE Trans. Electron Devices*, vol. 60, no. 10, pp. 3071–3078, Oct. 2013, doi: [10.1109/TED.2013.2274730](https://doi.org/10.1109/TED.2013.2274730).
- [23] S. Arulkumaran, G. I. Ng, S. Vicknesh, H. Wang, K. S. Ang, C. M. Kumar, K. L. Teo, and K. Ranjan, "Demonstration of submicron-gate AlGaIn/GaN high-electron-mobility transistors on silicon with complementary metal-oxide-semiconductor-compatible non-gold metal stack," *Appl. Phys. Exp.*, vol. 6, no. 1, Jan. 2013, Art. no. 016501, doi: [10.7567/apex.6.016501](https://doi.org/10.7567/apex.6.016501).
- [24] H.-S. Lee, D. Seup Lee, and T. Palacios, "AlGaIn/GaN high-electron-mobility transistors fabricated through a Au-free technology," *IEEE Electron Device Lett.*, vol. 32, no. 5, pp. 623–625, May 2011, doi: [10.1109/LED.2011.2114322](https://doi.org/10.1109/LED.2011.2114322).
- [25] M. Piazza, C. Dua, M. Oualli, E. Morvan, D. Carisetti, and F. Wyczisk, "Degradation of TiAlNiAu as ohmic contact metal for GaN HEMTs," *Microelectron. Rel.*, vol. 49, nos. 9–11, pp. 1222–1225, Sep. 2009, doi: [10.1016/j.microrel.2009.06.043](https://doi.org/10.1016/j.microrel.2009.06.043).
- [26] A. Messina, U. Meirav, and H. Shtrikman, "Refractory metal-based low-resistance ohmic contacts for submicron GaAs heterostructure devices," *Thin Solid Films*, vol. 257, no. 1, pp. 54–57, Feb. 1995, doi: [10.1016/0040-6090\(94\)06346-x](https://doi.org/10.1016/0040-6090(94)06346-x).
- [27] X. Kong, K. Wei, G. Liu, and X. Liu, "Role of Ti/Al relative thickness in the formation mechanism of Ti/Al/Ni/Au ohmic contacts to AlGaIn/GaN heterostructures," *J. Phys. D, Appl. Phys.*, vol. 45, no. 26, Jun. 2012, Art. no. 265101, doi: [10.1088/0022-3727/45/26/265101](https://doi.org/10.1088/0022-3727/45/26/265101).
- [28] F. Roccaforte, F. Iucolano, F. Giannazzo, A. Alberti, and V. Raineri, "Nanoscale carrier transport in Ti/Al/Ni/Au ohmic contacts on AlGaIn epilayers grown on Si(111)," *Appl. Phys. Lett.*, vol. 89, no. 2, Jul. 2006, Art. no. 022103, doi: [10.1063/1.2220486](https://doi.org/10.1063/1.2220486).
- [29] D. Marcon and S. Decoutere, "Reliability analysis of permanent degradations on AlGaIn/GaN HEMTs," *IEEE Trans. Electron Devices*, vol. 60, no. 10, pp. 3132–3141, Oct. 2013, doi: [10.1109/TED.2013.2273216](https://doi.org/10.1109/TED.2013.2273216).
- [30] N. Wolff, T. Hoffmann, W. Heinrich, and O. Bengtsson, "Impact of drain-lag induced current degradation for a dynamically operated GaN-HEMT power amplifier," in *IEEE MTT-S Int. Microw. Symp. Dig.*, Jun. 2018, pp. 168–171, doi: [10.1109/MWSYM.2018.8439576](https://doi.org/10.1109/MWSYM.2018.8439576).